Campbell, H. D. (1983) *Anal. Lett. 16*, 1495-1507.
Campbell, H. D., & Young, I. G. (1983) *Biochemistry 22*, 5754-5760.
Chowdhry, V., & Westheimer, F. H. (1979) *Annu. Rev. Biochem. 48*, 293-325.
Crane, F. L., & Barr, R. (1971) *Methods Enzymol. 18*, 137-165.
Fleet, G. W. J., Knowles, J. R., & Porter, R. R. (1972) *Biochem. J. 128*, 499-508.
Guillory, R. J., & Jeng, S. J. (1977) *Methods Enzymol. 46*, 259-288.
Hennion, G. F., & Barrett, S. O. (1957) *J. Am. Chem. Soc. 79*, 2146-2148.
Höfle, G., Steglich, W., & Vorbrüggen, H. (1978) *Angew. Chem., Int. Ed. Engl. 17*, 569-583.
Jaworowski, A., Campbell, H. D., Poulis, M. I., & Young, I. G. (1981a) *Biochemistry 20*, 2041-2047.
Jaworowski, A., Mayo, G., Shaw, D. C., Campbell, H. D., & Young, I. G. (1981b) *Biochemistry 20*, 3621-3628.
Jeng, S. J., & Guillory, R. J. (1975) *J. Supramol. Struct. 3*, 448-468.
Kröger, A., & Klingenberg, M. (1973a) *Eur. J. Biochem. 34*, 358-368.
Kröger, A., & Klingenberg, M. (1973b) *Eur. J. Biochem. 39*, 313-323.
Lowry, O. H., Rosebrough, N. J., Farr, A. L., & Randall, R. J. (1951) *J. Biol. Chem. 193*, 265-275.
Markownikoff, W. (1890) *Justus Liebigs Ann. Chem. 153*, 228-259.
Mayer, H., & Isler, O. (1971) *Methods Enzymol. 18*, 182-213.
Neises, B., & Steglich, W. (1978) *Angew. Chem., Int. Ed. Engl. 17*, 522-524.
Paul, R., & Anderson, G. W. (1960) *J. Am. Chem. Soc. 82*, 4596-4600.
Schneider, H., Lemasters, J. J., & Hackenbrock, C. R. (1982) *J. Biol. Chem. 257*, 10789-10793.
Staab, H. A., & Mannschreck, A. (1962) *Chem. Ber. 95*, 1284-1297.
Wagner, A. F., Lusi, A., Shunk, C. H., Linn, B. O., Wolf, D. E., Hoffman, C. H., Erickson, R. E., Arison, B., Trenner, N. R., & Folkers, K. (1963) *J. Am. Chem. Soc. 85*, 1534-1535.
Wallace, B. J., & Young, I. G. (1977a) *Biochim. Biophys. Acta 461*, 75-83.
Wallace, B. J., & Young, I. G. (1977b) *Biochim. Biophys. Acta 461*, 84-100.
Young, I. G., Rogers, B. L., Campbell, H. D., Jaworowski, A., & Shaw, D. C. (1981) *Eur. J. Biochem. 116*, 165-170.
Yu, C.-A., & Yu, L. (1981) *Biochim. Biophys. Acta 639*, 99-128.
Yu, C.-A., & Yu, L. (1982) *Biochemistry 21*, 4096-4101.

Evidence for Nystatin Micelles in L-Cell Membranes from Fluorescence Photobleaching Measurements of Diffusion†

L. J. O'Neill, J. G. Miller, and N. O. Petersen*
Department of Chemistry, The University of Western Ontario, London, Ontario, N6A 5B7 Canada
Received April 24, 1985

ABSTRACT: Diffusion of a nitrobenzoxadiazole derivative of the polyene antibiotic nystatin in the membranes of L cells is found to depend on the concentration of nystatin in the membrane. Its diffusion coefficient measured by fluorescence photobleaching decreases hyperbolically as the concentration of nystatin is increased. This behavior is reproduced when the concentration of the derivative is increased. In contrast, diffusion of a nitrobenzoxadiazole derivative of a phospholipid is insensitive to the nystatin concentration under these conditions. The nystatin-specific diffusion changes can be understood if nystatin exists in a monomer–micelle equilibrium within the membrane but cannot be accounted for by binding or phase partitioning.

Nystatin is one of several polyene antibiotics used clinically as an antifungal agent (Hammond, 1977; Medoff et al., 1983). These drugs are known to be membrane-active agents which can induce K^+ leakage and cell lysis in yeast, erythrocytes, and mammalian cells including murine L cells (Gale, 1974). A large body of work with model membranes [reviewed by Hammond (1977)] has led to the suggestion that polyene antibiotics, such as nystatin and amphotericin B, associate with sterols in the membrane to form transmembrane pores (de Kruijff & Demel, 1974; van Hoogevest & de Kruijff, 1978).

The polyene antibiotics produce a variety of effects on mammalian cells in vivo and in culture (Medoff et al., 1983) perhaps involving more than one mechanism. Accordingly, we have become interested in characterizing in more detail the interactions of polyene antibiotics with membranes of living cells. Measurements of diffusion of membrane components represent one approach to studying their dynamic interactions through, for example, binding to slowly moving structures (Elson & Reidler, 1979). We have recently reported the synthesis and characterization of nitrobenzoxadiazole derivatives of amphotericin B (Petersen, 1983), nystatin, and pimaricin (Petersen, 1985) and have characterized an interesting and potentially useful intramolecular fluorescence energy transfer process in these derivatives (Petersen, 1985). In this paper, we present diffusion data which provide evidence for

† This work was supported by the Natural Sciences and Engineering Research Council of Canada (Grant U109), by the National Institutes of Health (NCI Grant CA14554 and NIAID Grant AI16228), and by the Academic Development Fund of The University of Western Ontario.

0006-2960/86/0425-0177$01.50/0

formation of micelles of nystatin within the membranes of living cells.

Experimental Procedures

Materials. *N*-(4-Nitro-2,1,3-benzoxadiazolyl)-6-aminohexanoyl derivatives of nystatin (NBD-Nys)[1] and amphotericin B (NBD-AmB) have been characterized (Petersen, 1983, 1985). A nitrobenzoxadiazole derivative of phosphatidylethanolamine from egg yolk lipids (NBD-PE) was purchased from Avanti (Birmingham, AL; catalog no. 810118, lot no. FPE-24). Tissue culture medium was kindly provided by the tissue culture facility in the Department of Biochemistry at The University of Western Ontario. Medium 199 (without phenol red) and gentamicin were obtained from Gibco, Canada. Nystatin was purchased from Sigma (St. Louis, MO). Other chemicals were analytical-grade reagents (Fisher).

Cell Cultures. Murine L cells (originally provided by Professor W. F. Flintoff, Department of Microbiology and Immunology, U.W.O.) were cultured in medium 199 containing 10% horse serum and 36 mg/500 mL gentamicin and passed twice a week. For experiments, L cells were trypsinized and plated on 22 × 22 mm sterile glass cover slides (Canlab) contained in 35-mm-diameter tissue culture dishes (Falcon). Cells were plated at 10^5 cells per dish 48 h before use and incubated at 37 °C in a 5% CO_2, 100% relative humidity incubator. Precautions were taken to standardize the growth conditions since the sensitivity to polyene antibiotics depends on the stage of growth (Gale, 1974).

Sample Preparations. In preparation for experiments, the cells were rinsed with phosphate-buffered saline (PBS) several times, and 2 mL of Hepes-buffered medium 199 without phenol red (25 mM Hepes, pH 7.4) was added. Appropriate volumes of NBD-Nys, NBD-PE, or nystatin were added from 1.0 mg mL^{-1} solutions in dimethylformamide (DMF) which had been stored at −5 °C in the dark under a N_2 atmosphere for no more than 10 days. Following incubation at 37 °C for the selected time, the cells were again rinsed several times with PBS and transferred to a clean 35-mm-diameter tissue culture dish containing 3 mL of Hepes-buffered medium 199.

Fluorescence Photobleaching Recovery (FPR). FPR measurements were performed by using equipment described previously (Petersen & Elson, 1986) and were analyzed by curve-fitting procedures adapted from those reported (Petersen et al., 1984). In these experiments, the 488-nm line of an argon ion laser was focused with external optics and a 40× water immersion objective to a beam width of 1.4 μm. The laser power at the source was adjusted to 30 mW and attenuated to less than a microwatt at the sample. Photobleaching was achieved with 50–100-ms exposures to a 1–10-mW beam parfocal and concentric with the monitor beam. At each concentration, five to eight morphologically similar cells were studied. Five to ten measurements were made on each cell and averaged. At a given concentration, the total number of measurements was in the range from 20 to 80. For several concentrations, the experiments were repeated with good reproducibility, and the data reported represent overall averages of *N* bleaches. Standard statistical analyses were employed to calculate standard errors of the mean (SEM) at the 99% confidence level for two-tailed analysis. All diffusion (*D*) measurements were made at 24 ± 2 °C and are reported as *D* ± SEM (*N*).

Table I: Diffusion Coefficients (*D*) and Mobile Fractions (X_m) of NBD-Nys as a Function of Nystatin Preincubation Time (t_p) and Relative NBD-Nys–Nystatin Concentrations

$C_{NBD\text{-}Nys}$[a]	C_{Nys}[a]	t_p (min)	D ± SEM[b]	X_m ± SEM	N[c]
13.2	13.3	0	1.9 ± 1.1	0.66 ± 0.04	31
		10	0.6 ± 0.1	0.79 ± 0.07	25
		20	0.9 ± 0.2	0.70 ± 0.05	18
15.6	10.5	0	2.4 ± 0.4	0.77 ± 0.04	47
		10	1.9 ± 0.5	0.71 ± 0.05	52
		20	2.4 ± 1.0	0.79 ± 0.05	30
		50	3.6 ± 1.0	0.81 ± 0.04	39
18.0	9.1	0	6.6 ± 1.0	0.73 ± 0.03	43
		10	5.6 ± 0.6	0.76 ± 0.04	41
		20	4.8 ± 0.8	0.74 ± 0.04	50

[a] Solution concentrations in micrograms per milliliter. [b] Diffusion coefficient (*D*) and standard error of the mean (SEM) in units of 10^{-13} m^2 s^{-1}. [c] Number of bleaches.

Results

The fluorescence intensity measured in small regions of the surface of L cells exposed to varying concentrations of NBD-Nys increases linearly with solution concentration over the range from 5 to 50 μg mL^{-1}. There is no evidence for saturation. In principle, it is possible to calibrate the fluorescence intensity counts in terms of the density of NBD-Nys molecules per square micrometer provided the illumination geometry, the fluorescence quantum yield, and instrumental attenuation factors are known (Koppel et al., 1976; Petersen & McConnaughey, 1981). In this system, the membrane concentration of NBD-Nys varies from about 5 × 10^3 to 5 × 10^4 molecules/μm^2 when the solution concentration varies from 5 to 50 μg mL^{-1}. These numbers are approximate estimates because among other things the quantum yield for fluorescence of NBD-Nys is very sensitive to the solvent environment (Petersen, 1985). For this reason, we present the data in this paper in terms of the solution concentration rather than the membrane concentration, bearing in mind that the two are linearly related.

It is known that the effects of polyene antibiotics on cell membrane permeability can depend on both solution concentration and time of incubation in complex ways (Hammond, 1977; Gale, 1974). Table I shows that the diffusion of NBD-Nys in cells which have been preincubated with nystatin for various periods and then coincubated with NBD-Nys for 10 min depends on both the preincubation time and the relative concentration of NBD-Nys and Nys. The variation in diffusion coefficient is complex, and the larger values at long times of incubation at higher relative nystatin concentrations suggest that complicated kinetic processes may be involved. Thus, to compare the effects of nystatin on the diffusion of NBD-Nys and NBD-PE, a 10-min preincubation with nystatin was used here to maintain a near constant set of conditions.

In our experiments, the total volume of DMF in the incubation solution varies, but control experiments show that the NBD-Nys diffusion in cells exposed to 5 μg mL^{-1} NBD-Nys and an additional 25 μL of DMF remains high [D = (7.9 ± 1.5) × 10^{-13} m^2 s^{-1} (38)]. The amount of DMF and the choice of DMF as a solvent do not affect the diffusion measurements in this system. When NBD-PE is added in DMF, D = (2.0 ± 0.4) × 10^{-13} m^2 s^{-1} (104), and when it is added in 95% ethanol solutions, D = (1.9 ± 0.2) × 10^{-13} m^2 s^{-1} (31).

Figure 1 compares the diffusion coefficients of NBD-Nys (5 μg mL^{-1}) and NBD-PE (2 μg mL^{-1}) measured after preincubation with various nystatin concentrations. Three important general observations can be made from these data:

[1] Abbreviations: NBD-Nys, [*N*-(4-nitro-2,1,3-benzoxadiazolyl)-6-aminohexanoyl]nystatin; NBD-PE, *N*-(4-nitro-2,1,3-benzoxadiazolyl)-phosphatidylethanolamine; PBS, phosphate-buffered saline; DMF, dimethylformamide; FPR, fluorescence photobleaching recovery; SEM, standard error of the mean; cmc, critical micelle concentration; Hepes, *N*-(2-hydroxyethyl)piperazine-*N*′-2-ethanesulfonic acid.

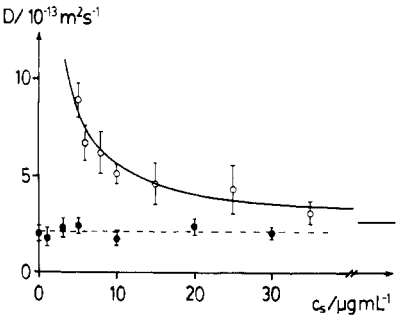

FIGURE 1: Variation in diffusion coefficient, D, for 5 μg mL^{-1} NBD-Nys (○) and 2 μg mL^{-1} NBD-PE (●) as a function of total solution concentration (C_S) of polyene antibiotic (NBD-Nys + nystatin). The errors are indicated as the standard error of the mean at the 99% confidence level for two-tailed tests. The solid line is the best-fit hyperbolic curve through the data (see also Figure 2). The asymptotic limit is indicated as a solid horizontal line. The dashed line indicates the average value of the NBD-PE diffusion coefficient. Each data point is the average of at least 30 bleaches and as many as 100–160 bleaches in some cases.

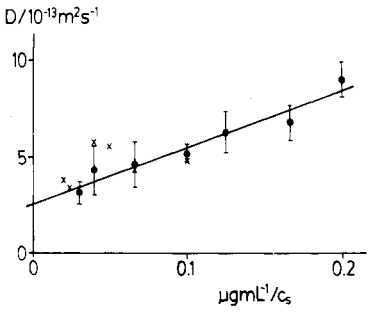

FIGURE 2: Variation in diffusion coefficient, D, for 5 μg mL^{-1} NBD-Nys (●) as a function of the inverse of the total solution concentration ($1/C_S$) of polyene antibiotic (NBD-Nys + nystatin). The solid line is the best-fit least-squares line through the data. The errors are the standard error of the mean (see Figure 1). These data are the same as in Figure 1. The diffusion coefficients at various concentrations of NBD-Nys in the absence of nystatin are indicated by (×) for comparison. Here C_S refers to the NBD-Nys concentration.

the diffusion coefficient of NBD-PE is independent of nystatin concentration [total average $D = (2.1 \pm 0.1) \times 10^{-13}$ m^2 s^{-1} (349)]; the diffusion coefficient of NBD-Nys decreases asymptotically toward a value less than 3×10^{-13} m^2 s^{-1} as the concentration of nystatin is increased; the diffusion of NBD-Nys is always more rapid than that of NBD-PE under these conditions. It should be noted that NBD-Nys and NBD-PE diffusion measurements were done in parallel as a function of nystatin concentration so that at a given nystatin concentration the experimental conditions were identical. The measurements at zero nystatin concentration are particularly important for the interpretation of the results, and therefore, more experiments were performed (N = 163 for NBD-Nys and N = 104 for NBD-PE).

Interpretation of the diffusion coefficient changes specific to NBD-Nys, in terms of a monomer–micelle equilibrium within the membrane, predicts that the diffusion coefficient should vary hyperbolically with concentration (vide infra). Hence, D should increase linearly when plotted as a function of $1/c$. Figure 2 illustrates this linear relationship for NBD-Nys diffusion. The solid line in Figure 2 represents the best-fit line through the data [slope = $(2.8 \pm 0.6) \times 10^{-12}$ m^2 s^{-1} μg^{-1} mL; intercept = $(2.6 \pm 0.7) \times 10^{-13}$ m^2 s^{-1}; r = 0.968]. The corresponding best-fit hyperbolic curve has been drawn through the data in Figure 1 along with the asymptotic limit of $D = 2.6 \times 10^{-13}$ m^2 s^{-1}.

Figure 2 also shows the variation in the NBD-Nys diffusion coefficient as a function of the inverse NBD-Nys concentration. These values are slightly more scattered but parallel the changes observed when the nystatin concentration is varied, suggesting that similar effects are induced in the membrane by nystatin and its nitrobenzoxadiazole derivative at comparable concentrations.

The fractions of mobile NBD-Nys or NBD-PE were minimally affected by preincubation with nystatin in these experiments but were consistently lower than unity because of unaccounted background fluorescence including autofluorescence. There is no evidence from the fluorescence microscopy that the dye is internalized in vesicular structures. For NBD-Nys, $X_m = 0.74 \pm 0.02$ while for NBD-PE $X_m = 0.80 \pm 0.02$ when all the data are considered. These values are typical of lipid dyes in cultures cells (Jacobson et al., 1981).

Discussion

The effect of chemical kinetics on the interpretation of fluorescence correlation spectroscopy (FCS) and fluorescence photobleaching recovery (FPR) measurements has been discussed in general (Magde & Elson, 1974; Icenogle & Elson, 1983a,b; Elson & Reidler, 1980). In the limit of slow kinetics, FPR should reveal superpositions of separately diffusing species (van Zoelen et al., 1983; Petersen & Elson, 1986). Multiple and even two diffusion coefficients can be difficult to extract because of the slow recovery of the fluorescence at long times unless the diffusion coefficients are very different ($D_1/D_2 \gtrsim 10$). In this system, all the recovery curves were well fitted with single diffusion coefficient analysis which indicates either that the difference in diffusion coefficients is small ($D_1/D_2 \lesssim 3$) or that a single mean diffusion coefficient is dominant. The latter will occur in the limit of fast chemical kinetics (Elson & Reidler, 1979), and the resultant observed diffusion coefficient is the weighted average of the diffusion coefficients of the species in chemical equilibrium. In general, for a fluorescent probe in two environments where it can diffuse either rapidly at D_R or slowly at D_S, the observed diffusion coefficient, D_{obsd}, is given by

$$D_{obsd} = f_R D_R + f_S D_S \quad (1)$$

where f_R and f_S are the mole fractions of the probe in the rapid and slow environments ($f_R + f_S = 1$). The diffusion coefficient is therefore concentration dependent if the mole fractions vary with concentration. In this model, the observed decrease in diffusion coefficient of NBD-Nys (Figure 1) must reflect an increase in the mole fraction of slowly moving NBD-Nys at higher concentrations. We believe this can be understood by a monomer–micelle equilibrium in the cell membrane but not by binding or phase partitioning.

Monomer–Micelle Model. Amphotericin B, and by analogy nystatin, is believed to associate with sterols in cell and model membranes to form ion-conductive pores (de Kruijff & Demel, 1974). Irrespective of the detailed structure and composition of such aggregates, the implication is that they are thermodynamically stable systems whose stability is derived in part from the amphiphilic properties of the polyene antibiotic. They can be thought of as inverted micelles with properties analogous to micelles in solution systems (Tanford, 1973). An important feature of micelles is that there exists a concentration [the critical micelle concentration (cmc)] below which virtually no micelles can form and above which almost all additional monomers form micelles. We suggest that nystatin, and perhaps other polyene antibiotics, interacts with cell membranes to form micelles *within* the lipid bilayer, but only at concentrations exceeding the cmc in the membrane.

Figure 3 illustrates schematically the effect of a monomer–micelle equilibrium on the mean diffusion coefficient, D.

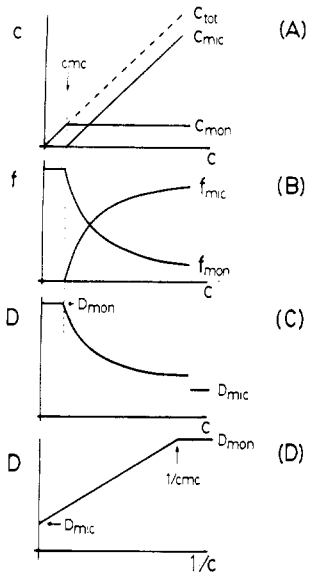

FIGURE 3: Schematic representation of the effects of a monomer–micelle equilibrium on (A) the concentration of monomers as monomers (C_{mon}) or in micelles (C_{mic}), (B) the mole fraction of monomers as monomers (f_{mon}) or in micelles (f_{mic}), and (C) the mean observed diffusion coefficient, D. Each of these is shown as a function of total monomer concentration. The diffusion coefficient is shown as a function of inverse concentration in (D). The functions are discontinuous at the critical micelle concentration (cmc) as indicated. It is evident that (C) and (D) are schematic representations of Figures 1 and 2.

At concentrations below the cmc, the concentration of monomers in the membrane increases linearly with the total solution concentration. Above the cmc, the concentration of nystatin in micelles in the membrane increases linearly with the total solution concentration while the monomer concentration remains constant (Figure 3A). Below the cmc, the mole fraction of nystatin as monomers is unity, and by eq 1, the observed diffusion coefficient equals the monomer diffusion coefficient, D_{mon}. Above the cmc, the mole fraction of nystatin as monomers decreases while that of nystatin in micelles increases (Figure 3B). It is possible to rewrite eq 1 as

$$D_{obsd} = f_{mon}D_{mon} + f_{mic}D_{mic} = \frac{C_{mon}}{C_{tot}}D_{mon} + \frac{C_{mic}}{C_{tot}}D_{mic}$$

where C_{mon}, C_{mic}, and C_{tot} refer to the membrane concentrations of free monomers, of monomers in micelles, and of total monomers. In the linear region of the binding curve, these concentrations reflect the corresponding solution concentrations and hence

$$D_{obsd} = \frac{C_0^m}{KC_S}D_{mon} + \frac{KC_S - C_0^m}{KC_S}D_{mic} = \frac{C_0^m}{KC_S}(D_{mon} - D_{mic}) + D_{mic} \quad (2)$$

where $C_{mon} = C_0^m$ = cmc of nystatin in the membrane, C_S is the solution concentration of nystatin, and K is a partition coefficient which permits converting membrane concentrations to solution concentrations ($C_{tot} = KC_S$). Equation 2 predicts a hyperbolic relationship between D_{obsd} and C_S (Figure 3C) and a linear relationship between D_{obsd} and $1/C_S$ (Figure 3D) at concentrations above the cmc. Figure 2 shows the fit of the observed diffusion coefficient to the form of eq 2 and yields an in-membrane micellar diffusion coefficient of $D_{mic} = 2.6 \times 10^{-13}$ m^2 s^{-1}.

From the data at hand, it is difficult to calculate either C_0^m or the monomer diffusion coefficient. We cannot measure diffusion coefficients at lower NBD-Nys concentrations since the fluorescence intensity approaches the limits of our instrumental sensitivity. The largest diffusion coefficients measured for lipid probes in cell membranes at 25 °C are about 10^{-12} m^2 s^{-1} (Jacobson et al., 1981). If we assume that the nystatin monomer diffusion coefficient approaches this limit, we can estimate the cmc at a solution concentration of 3.8 μg mL^{-1} corresponding to a membrane concentration of about (3–4) $\times 10^3$ nystatin molecules/μm^2. The cmc then occurs at nystatin:lipid molar ratios of about 1:300. In model membrane systems, ion leakage occurs at amphotericin B:lipid molar ratios around 1:1000 or 1:3000 (Vertut-Croquin et al., 1983). Considering the approximations in the estimate of the cmc, the agreement is encouraging and supports the proposal that micelle formation is linked to ion leakage. K^+ leakage in L cells occurs rapidly at solution concentrations above about 5–10 μg mL^{-1} but depends on the time of incubation (Gale, 1974). We have initiated K^+ leakage studies with our systems to substantiate this link between ionic leakage and micelle formation.

Most of the variation in diffusion measurements on living cells arises from heterogeneity in the cell population. Specifically, if uptake of drug depends on the cell cycle (Gale, 1974), the cell to cell variation of the effect on diffusion could explain the larger spread of data for NBD-Nys than for NBD-PE. For this reason, we suspect that the monomer–micelle equilibrium could be studied in more detail in selected model membrane systems. Such studies would also clarify whether the equilibrium is affected by cell membrane components other than phospholipids and sterols.

Binding or Partitioning. The observed diffusion coefficient could be modulated by binding or phase partitioning. In the case of binding to, for example, proteins (Elson & Reidler, 1979):

$$D_{obsd} = f_F D_F + f_B D_B \quad (3)$$

where the subscripts F and B refer to free (rapidly moving) and bound (slowly moving) polyene. In the linear region of binding, the fraction bound is constant while saturation causes f_B to decrease and thus D_{obsd} to increase. This is contrary to the observed trend, and binding can be excluded. A Scatchard plot is a more quantitative test for simple binding (n equivalent and independent sites) in which the linear relation

$$C_B/C_F = S/K - C_B/K \quad (4)$$

is expected when S is the total concentration of binding sites, K is the equilibrium constant, and C denotes concentration. In terms of diffusion coefficients, we can express (from eq 3) $C_B/C_F = (D_F - D_{obsd})/(D_{obsd} - D_B)$ and $C_B/C_{tot} = (D_F - D_{obsd})/(D_F - D_B)$, and eq 4 transforms to

$$\frac{D_F - D_{obsd}}{D_{obsd} - D_B} = \frac{S}{K} - \frac{C_{tot}}{K}\left(\frac{D_F - D_{obsd}}{D_F - D_B}\right) \quad (5)$$

Irrespective of the specific values of D_F and D_B, the decreasing diffusion coefficients observed for NBD-Nys with increasing nystatin concentration will generate a negative binding constant. Thermodynamically, this does not make sense.

If the cell membrane consists of domains of different lipids with distinct viscosities, the partitioning of a fluorescent dye between these domains would affect the observed diffusion coefficient. In that case, the ratio of the concentrations in each domain is given by the partition coefficient, which is a constant. A decrease in the observed diffusion coefficient implies either an association reaction in the less fluid domains or an increase in the fraction of lipid in those domains. The latter can be

excluded, because a decrease in the fraction of more fluid domains and an increase in that of the less fluid domains should decrease the NBD-PE diffusion correspondingly and would not be specific for the NBD-Nys diffusion. The data do not exclude the possibility that micelle formation occurs preferentially in less fluid domains, but the monomer–micelle equilibrium model does not require different domains in the membrane.

Relative Diffusion of NBD-Nys and NBD-PE. Figure 1 shows that the diffusion of NBD-Nys is always more rapid than that of NBD-PE. This is an enigma since the molecular dimensions of NBD-Nys and NBD-PE are quite similar. We can offer two possible explanations but do not have evidence to favor one over the other.

Bolard and co-workers (Bolard et al., 1980) have interpreted circular dichroism measurements of the interaction of amphotericin B with model membranes in terms of spectroscopically distinct species and have suggested that some of these are adsorbed on the surface of the membrane. Such surface-adsorbed molecules could diffuse more rapidly than the lipid in the membrane. The slower diffusion of NBD-nystatin at higher concentrations of nystatin could be a result of formation of complexes in the bilayer proper which diffuse at rates comparable to those of the lipid analogue. However, the change in partitioning between the surface and the bilayer must still be driven by an association equilibrium within the bilayer. Without such associations, there would be no concentration dependence of the partitioning and hence no change in observed diffusion coefficient.

Alternatively, if there are different lipid domains in the membrane, then nystatin and NBD-Nys could preferentially partition into the more fluid domains while NBD-PE distributes in both. The rapid diffusion of NBD-Nys at low concentrations then reflects the viscous properties of the more fluid regions, and the slower diffusion at higher concentrations reflects micelle formation (which could occur in either domain). The slow NBD-PE diffusion at all nystatin concentrations would indicate that a large fraction of the NBD-PE is partitioned into the less fluid phase, reflecting largely its viscous properties. This explanation is reasonable since the diffusion measurements were performed at ambient temperatures. One would predict that the ratio of NBD-Nys to NBD-PE diffusion should be smaller at the physiological temperature of 37 °C. We have recently acquired a temperature-controlled microscope stage which will permit testing this prediction.

Conclusions

The data presented in this report show that NBD-Nys diffusion, but not NBD-PE diffusion, is sensitive to the concentration of nystatin in L cells. The concentration dependence of the diffusion coefficient can be explained by a model in which there is a dynamic equilibrium between monomers and micelles of nystatin within the cell membrane. Simple binding or partitioning equilibria cannot account for the data without simultaneous association equilibria. NBD-Nys diffusion is more rapid than NBD-PE diffusion. This can be understood if there are domains of fluid membrane into which the NBD-Nys preferentially partitions or if the monomeric form of the polyene is adsorbed at the surface where it may diffuse more rapidly. In either case, the micelle structures would form within the membrane. Experiments in model membrane systems and with cells under different conditions may shed further light on the detailed mechanism whereby the observed diffusion coefficients are modulated by concentration.

Registry No. Nys-A_1, 34786-70-4; NBD-Nys-A_1, 96475-98-8.

References

Bolard, J., Seigneuret, M., & Boudet, G. (1980) *Biochim. Biophys. Acta 599*, 280.

de Kruijff, B., & Demel, R. A. (1974) *Biochim. Biophys. Acta 339*, 57.

Elson, E. L., & Magde, D. (1974) *Biopolymers 13*, 1.

Elson, E. L., & Reidler, J. A. (1979) *J. Supramol. Struct. 12*, 481.

Gale, E. F. (1974) *J. Gen. Microbiol. 80*, 4451.

Hammond, S. M. (1977) *Prog. Med. Chem. 14*, 106.

Icenogle, R. D., & Elson, E. L. (1983a) *Biopolymers 22*, 1919.

Icenogle, R. D., & Elson, E. L. (1983b) *Biopolymers 22*, 1949.

Jacobson, K., Hou, Y., Derzko, Z., Wojcieszyn, J., & Organisciak, D. (1981) *Biochemistry 20*, 5268.

Koppel, D. E., Axelrod, D., Schlessinger, J., Elson, E. L., & Webb, W. W. (1976) *Biophys. J. 16*, 1315.

Medoff, G., Brajtburg, J., Kobayashi, G. S., & Bolard, J. (1983) *Annu. Rev. Pharmacol. Toxicol. 23*, 303.

Petersen, N. O. (1983) *Spectrosc.: Int. J. 2*, 408.

Petersen, N. O. (1985) *Can. J. Chem. 63*, 77.

Petersen, N. O., & McConnaughey, W. B. (1981) *J. Supramol. Struct. Cell. Biochem. 17*, 213.

Petersen, N. O., & Elson, E. L. (1986) *Methods Enzymol.* (in press).

Petersen, N. O., Felder, S., & Elson, E. L. (1984) in *Handbook of Experimental Immunology* (Weir, D. M., Herzenberg, L. A., Blackwell, C. C., & Herzenberg, L. A., Eds.) Chapter 27, Blackwell Scientific Publications Ltd., Oxford.

Tanford, C. (1973) *The Hydrophobic Effect: Formation of Micelles and Biological Membranes*, Wiley-Interscience, New York.

van Hoogevest, P., & de Kruijff, B. (1978) *Biochim. Biophys. Acta 511*, 397.

vanZoelen, E. J. J., Tertoolen, L. G. J., & deLaat, S. W. (1983) *Biophys. J. 42*, 103.

Vertut-Croquin, A., Bolard, J., Chabbert, M., & Gary-Bobo, C. (1983) *Biochemistry 22*, 2939.